



# Geothermal Reservoir Simulation Analysis in Support of Electricity Co- Production Feasibility Study at the Blackburn Oil Field, Nevada

## Preprint

Kagan Kutun, Abra Gold, and Koenraad Beckers

*National Renewable Energy Laboratory*

*Presented at the 2024 Geothermal Rising Conference  
Waikoloa, Hawaii  
October 27-30, 2024*

**NREL is a national laboratory of the U.S. Department of Energy  
Office of Energy Efficiency & Renewable Energy  
Operated by the Alliance for Sustainable Energy, LLC**

This report is available at no cost from the National Renewable Energy  
Laboratory (NREL) at [www.nrel.gov/publications](http://www.nrel.gov/publications).

Contract No. DE-AC36-08GO28308

**Conference Paper**  
NREL/CP- 5700- 90827  
October 2024



# **Geothermal Reservoir Simulation Analysis in Support of Electricity Co- Production Feasibility Study at the Blackburn Oil Field, Nevada**

## **Preprint**

Kagan Kutun, Abra Gold, and Koenraad Beckers

*National Renewable Energy Laboratory*

### **Suggested Citation**

Kutun, Kagan, Abra Gold, and Koenraad Beckers. 2024. *Geothermal Reservoir Simulation Analysis in Support of Electricity Co-Production Feasibility Study at the Blackburn Oil Field, Nevada*. Golden, CO: National Renewable Energy Laboratory. NREL/TP- 5700- 90827. <https://www.nrel.gov/docs/fy25osti/90827.pdf>.

**NREL is a national laboratory of the U.S. Department of Energy  
Office of Energy Efficiency & Renewable Energy  
Operated by the Alliance for Sustainable Energy, LLC**

This report is available at no cost from the National Renewable Energy Laboratory (NREL) at [www.nrel.gov/publications](http://www.nrel.gov/publications).

Contract No. DE-AC36-08GO28308

**Conference Paper**  
NREL/CP- 5700- 90827  
October 2024

National Renewable Energy Laboratory  
15013 Denver West Parkway  
Golden, CO 80401  
303-275-3000 • [www.nrel.gov](http://www.nrel.gov)

## NOTICE

This work was authored by the National Renewable Energy Laboratory, operated by Alliance for Sustainable Energy, LLC, for the U.S. Department of Energy (DOE) under Contract No. DE-AC36-08GO28308. Funding provided by the U.S. Department of Energy Office of Energy Efficiency and Renewable Energy Geothermal Technologies Office. The views expressed herein do not necessarily represent the views of the DOE or the U.S. Government.

This report is available at no cost from the National Renewable Energy Laboratory (NREL) at [www.nrel.gov/publications](http://www.nrel.gov/publications).

U.S. Department of Energy (DOE) reports produced after 1991 and a growing number of pre-1991 documents are available free via [www.OSTI.gov](http://www.OSTI.gov).

*Cover Photos by Dennis Schroeder: (clockwise, left to right) NREL 51934, NREL 45897, NREL 42160, NREL 45891, NREL 48097, NREL 46526.*

NREL prints on paper that contains recycled content.

# Geothermal Reservoir Simulation Analysis in Support of Electricity Co-Production Feasibility Study at the Blackburn Oil Field, Nevada

Kagan Kutun\*\*, Abra Gold\*, and Koenraad Beckers\*

\*National Renewable Energy Laboratory (NREL), \*\*Colorado School of Mines (work performed at NREL)

## Keywords

*Resource characterization, Reservoir Simulation, Co-production, Wells of opportunity, Blackburn Nevada, Organic Rankine cycle*

## ABSTRACT

Geothermal electricity co-production is a viable option for oil reservoirs producing large water cuts with elevated wellhead temperatures. Repurposing existing oil wells significantly reduces initial investment costs historically associated with geothermal resource utilization. The National Renewable Energy Laboratory (NREL), partnering with Gradient Geothermal, Inc. (formerly known as Transitional Energy) and Grant Canyon Oil and Gas, has been tasked to evaluate the feasibility of geothermal electricity co-production at the Blackburn Oil Field with Organic Rankine Cycle (ORC) generators. The Devonian steady-state reservoir has historically been producing high water cuts of 240°F (115.6°C) observed at the wellhead without documented pressure drawdown or thermal breakthrough. An estimated initial reservoir temperature of approx. 260°F (126.7°C) has been observed in the field and history-matched in a wellbore production analysis and reservoir simulation. Our objective was to develop a conceptual geological model of the subsurface, simulate a natural-state reservoir, model production scenarios, and complete a technical feasibility analysis to accomplish this task. Through extensive modeling and the use of available proprietary and public data, it was possible to simulate three scenarios that indicated minimal thermal decline over the duration of a simulated ten-year production and re-injection scheme.

## 1. Introduction

The Wells of Opportunity: Nevada (WOO Nevada) initiative aims to generate electricity at the Blackburn Field using the co-produced waters associated with the field's oil production. Blackburn Field is an oil field situated in Sections 7 and 8 of Township 27N Range 52E in northern Eureka County, Nevada. The field is in Pine Valley, approximately 45 miles ESE of Elko, NV.

Historical production records (NDOM 2023) indicate that from 1982 to 2022, Blackburn Field yielded 4.3 million barrels of oil and 43.5 million barrels of water. This resulted in an overall cumulative water-to-oil ratio of 91%. In 2022, the annual water cut was 98.98% (Kutun et al., 2023). The reservoir is a naturally fractured reservoir with a strong hydraulic drive, where water naturally recharges the reservoir. Wells historically drilled into the fractured Nevada dolomite



reservoir were typically completed at the shallowest (upper) depths to mitigate water encroachment from below.

An overview of the Blackburn Field wells is presented in Figure 1. Blackburn No. 12, 20, and 21 are three candidate injectors; Blackburn No. 4, 16, 18, 19, and 22 are candidate producers for the WOO Nevada project. Bucy No. 1 is also a candidate injection well located NNW of Blackburn No. 12.



**Figure 1: Map showing the locations of the Blackburn project co-production candidate wells.**

## **2. Geological Modeling**

The lithologies in the Blackburn field are, in stratigraphic order: the target reservoir Devonian Nevada dolomite, the reservoir-overlying Chainman shale capping layer (deposited post-Antler orogeny), the late Cretaceous quartz monzonite pluton that intruded during a 300 Ma unconformity, the Oligocene Indian Wells tuff, the Oligocene-Miocene lacustrine and conglomerate Humboldt, the Miocene basalt sill, the post-Miocene Hay Ranch (valley fill), and overlying alluvium (Flanigan 1994; Hulen et al. 1990; Scott & Chamberlain 1988). The quartz

monzonite pluton is referred to as the basement because it is the first metamorphic formation underlying the target Devonian reservoir.

A stratigraphic column with associated lithological descriptions is provided below in Figure 2. Formation tops from well completion reports and logs (hosted online by NBMG 2023), Taverna (2019), and our own interpretation (where no data were available), were honored as our primary data source in the creation of this conceptual model.

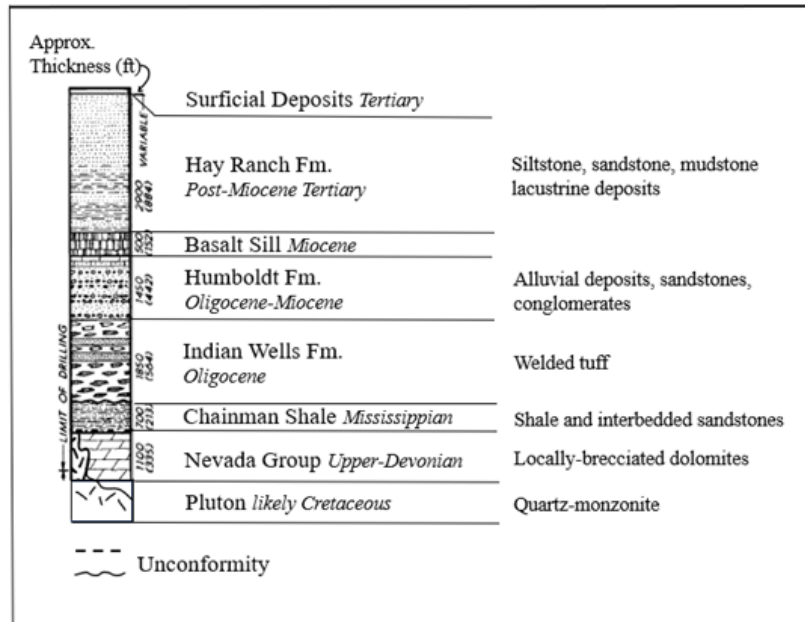


**Figure 2: Stratigraphic column and description of formations in the Blackburn Field subsurface, adapted from Hulen et al. 1990.**

The crust in this depositional basin is thinner than in other regions of the United States. This phenomenon is attributed to extensional plate tectonics. Extension causes fault dilation, allowing for fluid to flow in larger volumes along intricate fracture and fault pathways. An elevated thermal gradient is observed through the subsurface at the Blackburn Oil Field. It is likely that the heat source for the resource is deep-seated (Hulen et al. 1990). Geothermal fluids rise from depth along fault intersections. Dilated faults also facilitate secondary permeability. Many of the dilated faults in the Blackburn Field subsurface may have been infilled with sedimentary overburden. Future tracer research will offer further insight regarding fault permeability.

In the development of a 3D conceptual geological model, the cross-sections from Hulen et al. (1990) were utilized because they offered NNE and ENE views of the subsurface, whereas other publications did not offer as in-depth an interpretation. Determination of the quartz monzonite pluton contact is variable throughout the publications, because only two wells within the model area struck the pluton: Blackburn No. 1 and No. 6. The basement map from Scott & Chamberlain (1988) showing the quartz monzonite and Devonian surfaces was utilized in addition. As more data became available, the model evolved (Gold et al. 2024).

The next available data source utilized to influence model construction was a time-evolved structural fault map interpreted from a legacy seismic survey that was acquired in previous years (Flanigan, with modifications by the Blackburn field operator). This map was compared to

observed surface structures to provide a level of certainty in fault locations at depth (Gold et al. 2024). For numerical modeling purposes, faults were not extended beyond the top contact of the capping shale layer. All data sources were combined, with more confidence placed in the time-interpreted structural fault map, in the final version of the conceptual geological model and target reservoir contour surface (Figure 3 and Figure 4). The model boundaries were extended to the north and west to facilitate numerical simulation.

As formation tops data became sparse toward the outer boundaries of the model, the contacts were interpreted. Trends in the data were extrapolated from formation top data-dense clusters outward toward the less populated areas in the model.

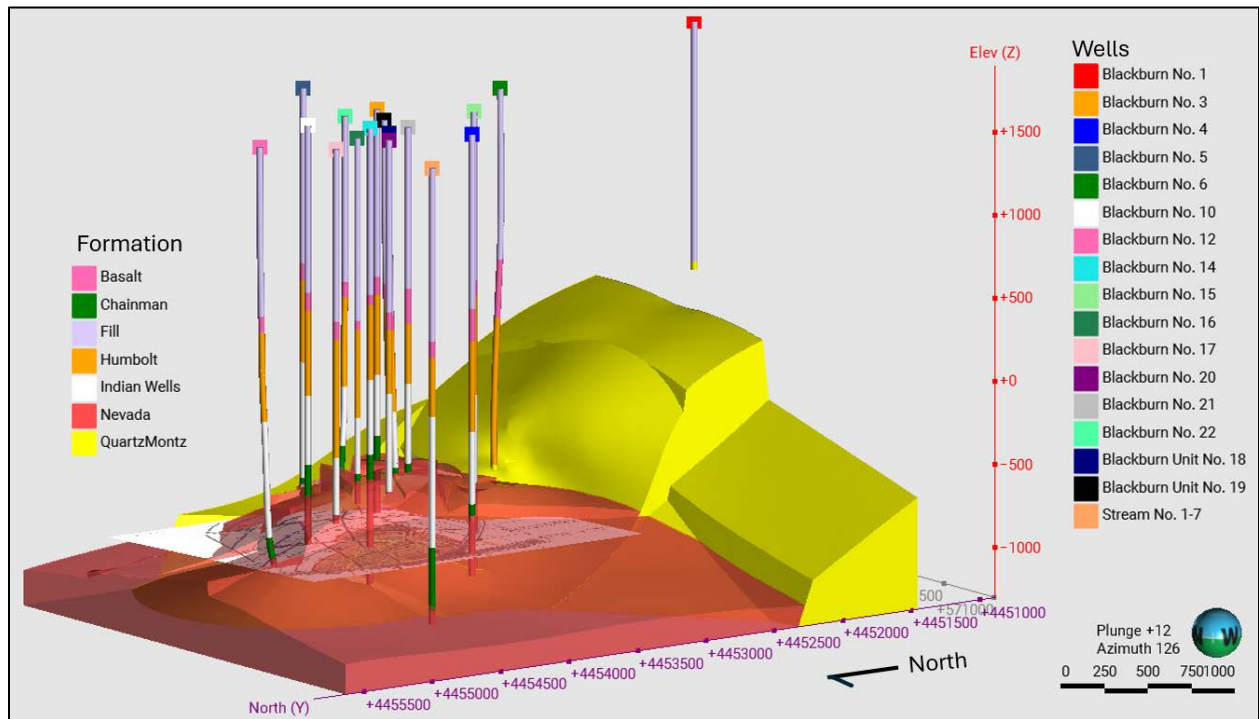


**Figure 3: 3D conceptual geological model of the Blackburn Oil Field Nevada dolomite (red) reservoir and underlying quartz monzonite (yellow), with boundaries extended laterally to the north and east.**



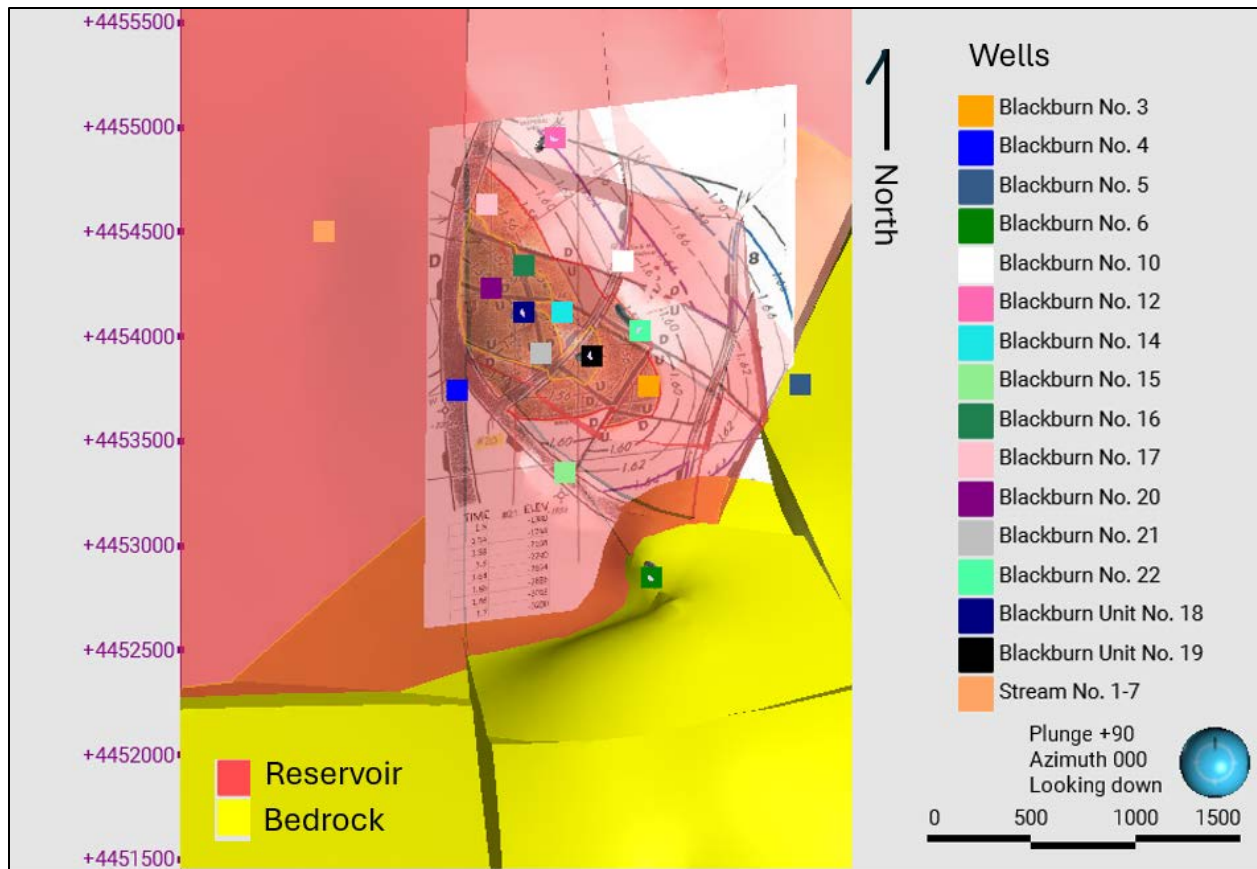


Figure 4: Well locations at depth imposed on the geological model of the reservoir and the basement, underlain by structural illustration data. The model extents have been edited to exclude Blackburn No. 1 because of reservoir termination prior to the well.

### 3. Reservoir Modeling

To numerically model the reservoir, the reservoir simulator VOLSUNG Brynhild was utilized. The simulator grid was populated with rock thermophysical properties, flow properties, and boundary conditions to reflect the Blackburn Field subsurface conditions.

The reservoir modeling study consisted of two parts. In the first part, a static reservoir model was created to match the temperature observations obtained from various sources. The purpose of the static modeling was to calibrate the numerically modeled reservoir domain to capture the natural state found in the system. In the second part, the calibrated model was subjected to different production scenarios to estimate the production temperatures for a ten-year project lifetime.

#### 3.1 Reservoir Model Input Parameters

##### 3.1.1 Thermophysical Properties

The thermal conductivity data,  $\lambda$  ( $\text{W m}^{-1} \text{K}^{-1}$ ), are mainly from lab analyses of rock types and formation samples obtained from the state of Nevada excepting basalt, the Humboldt, and the Hay Ranch (fill), for which no data points were found (UNR 2021; Blackwell & Steele 1989; Sass et



al. 1988). Specific formation data, if available, were used instead of averaging the range of rock type data measured from associated rocks obtained in the state of Nevada.

Measurements for formation heat capacities,  $c_p$  ( $\text{kJ kg}^{-1} \text{K}^{-1}$ ), and formation densities,  $\rho$  ( $\text{kg m}^{-3}$ ), from rock samples collected in the state of Nevada were not available. In this case, averages of ranges of general rock type-specific properties were utilized (Zhu et al. 2022; Schön, 2015, 2011; Waples 2004; Manger 1963). The thermophysical rock properties used in the model are presented in Table 1.

**Table 1: Thermophysical properties of formations in the Blackburn Oil Field. Properties were utilized for numerical modeling purposes.**

Formation	Designation	Thermal Conductivity	Heat Capacity	Density
		$\text{W m}^{-1} \text{K}^{-1}$	$\text{kJ kg}^{-1} \text{K}^{-1}$	$\text{kg m}^{-3}$
Quartz monzonite	Basement	3.05	0.879	2,640
Nevada Group	Reservoir	4.90	0.950	2,712
Chainman	Capping Layer	1.50	1.180	2,585
Indian Wells	Overlying Layer	1.74	0.943	2,416
Humboldt	Overlying Layer	1.82	1.109	2,525
Basalt	Overlying Layer	1.82	0.880	2,800
Hay Ranch & tertiary deposits (fill)	Overlying Layer	1.72	1.089	2,547

### 3.1.2 Flow Properties

The numerical model considered the flow of water only, i.e., no oil flow was modeled. The oil to water ratio (i.e. approximately 98% to 2%) was low, so excluding oil from the simulation did not influence the results significantly. This decision was determined in consideration of i) model software limitations (lack of water and oil equation of state), ii) relative permeability data unavailability, and iii) the observed 98% (or higher) water cut in the Devonian Nevada dolomite penetrating wells.

The layers above the Nevada Group were modeled as impermeable to fluid flow. The permeability of the Nevada dolomite and the quartz monzonite were chosen as 322 millidarcy based on the Drill Stem Test (DST) results reported for Blackburn well No. 18, October 12–13, 1992 (NBMG, 2023). The Nevada dolomite was set to have homogenous and isotropic permeability. The quartz monzonite basement was set to have homogenous permeability in the vertical direction only, i.e., the formation was incorporated as impermeable in horizontal directions.

Both the Nevada dolomite and the quartz monzonite basement were represented in the model as single porosity because no conclusive data was available to characterize the natural fracture and matrix permeability separately. The porosity of the two permeable formations were set as 5%. Pore compressibility values were set to  $7.25 \times 10^{-10} \text{ Pa}^{-1}$ . Thermal pore expansivity was not modeled.

The faults modeled in the geological modeling section of this work were not implemented in the numerical grid as no-flow barriers because no conclusive data was available. If these faults are in

fact no-flow barriers, omission of the faults in the numerical model will provide a worst-case scenario for thermal breakthrough concerns. Furthermore, the Blackburn field operator estimated that the faults are non-sealing at depth.

### 3.1.3 Boundary Conditions

Numerical boundary conditions were applied to the model on the grid top and grid bottom. The top boundary was set as a constant temperature at 55°F. This temperature was estimated from the spatially closest soil temperatures, which are values collected over 4 years at an elevation of 6,000 ft ASL approximately 80 mi away from the Blackburn Field (NRCS 2023).

The bottom boundary was constant temperature (at 273°F) and pressure (at 4,225 psi). Both the top and the bottom boundary conditions span the entire top and bottom surfaces of the grid, respectively. The side faces of the model were set as a no-flow boundary considering heat and fluid flow.

The temperature and pressure combination at the boundary conditions were chosen to impose a match in the reservoir model to multiple parameters. The observed Blackburn No. 18 well flowing field temperature data at the bottom of the wellbore, the overall temperature trends observed in the historical well log and DST temperature data, and the reservoir pressure estimation provided by Gradient Geothermal, Inc. were target parameters to be matched.

### 3.1.4. Grid Geometry

The grid layer spacing chosen is given in Table 2. The vertical layer spacing was chosen to provide higher resolution at the modeled reservoir layer and near the model’s top and bottom boundaries, while staying within the limits of our resources’ computational capabilities. Figure 5 presents a N-S cross-section of the grid.

**Table 2: Grid layer spacing used in this study. X and Y layers expand with given thicknesses in easterly and northerly directions, respectively. Z layers extend from the model’s top surface (5295 ft ASL) to the model’s bottom surface (-4300 ft ASL); i.e., layer 1 spanned from 5295 ft ASL to 5290 ft ASL, layer 86 spanned from -4100 ft ASL to -4300 ft ASL.**

<b>Extents</b>	<b>Layer Thickness, ft</b>	<b>Layers</b>	<b>Total Extent, ft</b>	<b>Total Layers</b>
<b>X</b>	200	52	10538	53
	138	1		
<b>Y</b>	400	34	13714	35
	114	1		
<b>Z</b>	5	1	9595	86
	122.5	4		
	250	2		
	400	6		
	200	16		
	50	56		
	200	1		

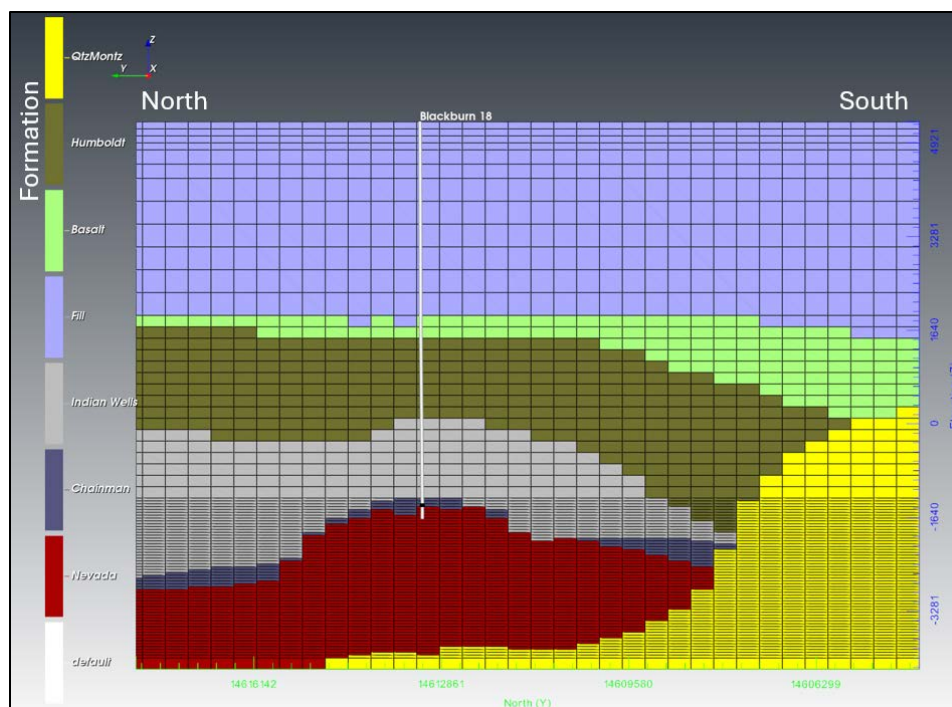


**Figure 5: North-south cross section of the constructed grid showing the lithology designation. The axis of the grid coincides with the location of Blackburn No. 18.**

### 3.2 Natural State Modeling

The objective of the static simulation was to calibrate the pressure and the temperature state of the model domain for dynamic production simulations. The static simulation was initialized with a temperature gradient of 0.030°F/ft and a pressure gradient of 0.44 psi/ft. Following the initialization, the simulation was run for 10,000 years, allowing the temperature and the pressure states to stabilize under the influence of the top and bottom boundary conditions. The relative temperature and pressure changes at the last time step of the simulation were  $2.3 \times 10^{-8} \text{ s}^{-1}$  and  $3.3 \times 10^{-12} \text{ s}^{-1}$ , respectively. These values indicated a reasonable numerical stabilization of the temperature and pressure distribution in the model domain.

The first targeted parameter match was to the temperature and pressure information obtained from the well flowing test conducted by the Blackburn field operator in August of 2023. In this test, the well flowing temperature and pressure profiles in the tubing were measured during stabilized flow. The observed well flowing temperature inside the tubing at 6,750 ft was 261.9°F; this temperature value was the target for the temperature match.

The observed well flowing pressure at the bottom of Blackburn No. 18 tubing (6,750' MD) was 3,040 psi. The test did not report a static reservoir pressure measurement. A static reservoir pressure estimate, which was based on the flow test, was provided by Gradient Geothermal, Inc., as 3,100 psi at the bottom-hole of Blackburn No. 18. This pressure estimate was the target pressure match for the static simulation run.

Figure 6 presents a N-S cross section of the temperature distribution, and Figure 7 presents a close-up screenshot of the temperature and pressure values obtained at the bottom of Blackburn 18 after

the static simulation was run. The average temperature of the four grid layers below the bottom of the tubing was observed as 261.7°F (in contrast to the 261.9°F observed in the flowing well test).

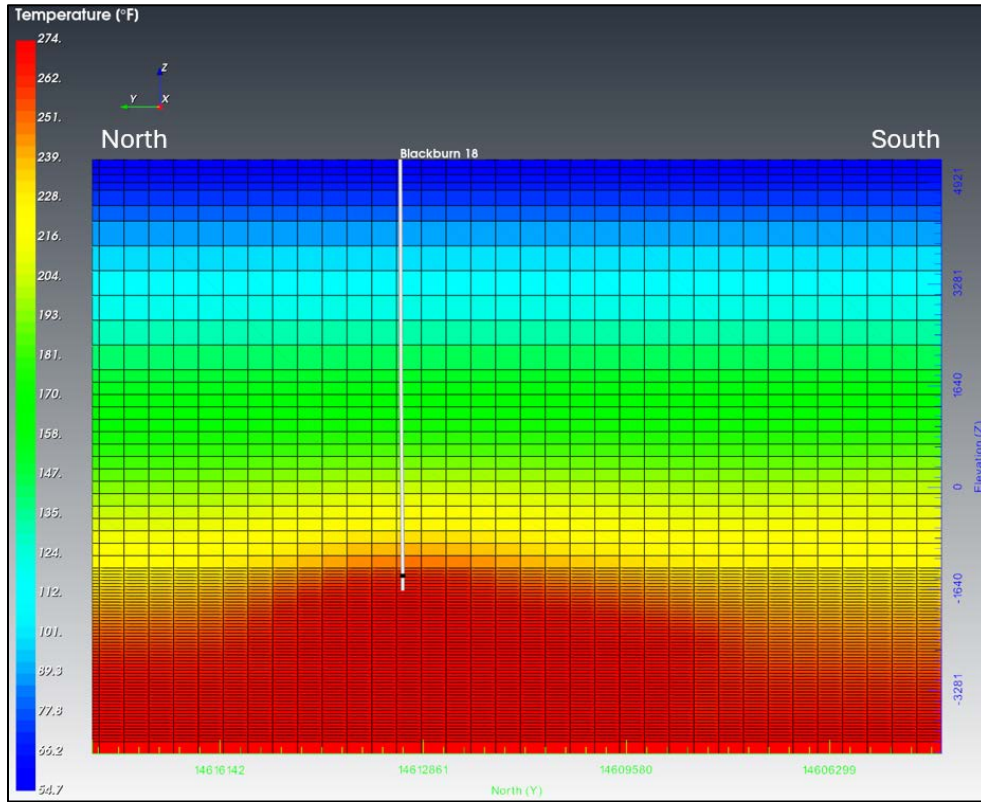


**Figure 6: N-S cross section of the stabilized natural state reservoir model. The cross-section line passes through the surface location of Blackburn 18. This well was not actively flowing during the stabilization of the natural-state model.**



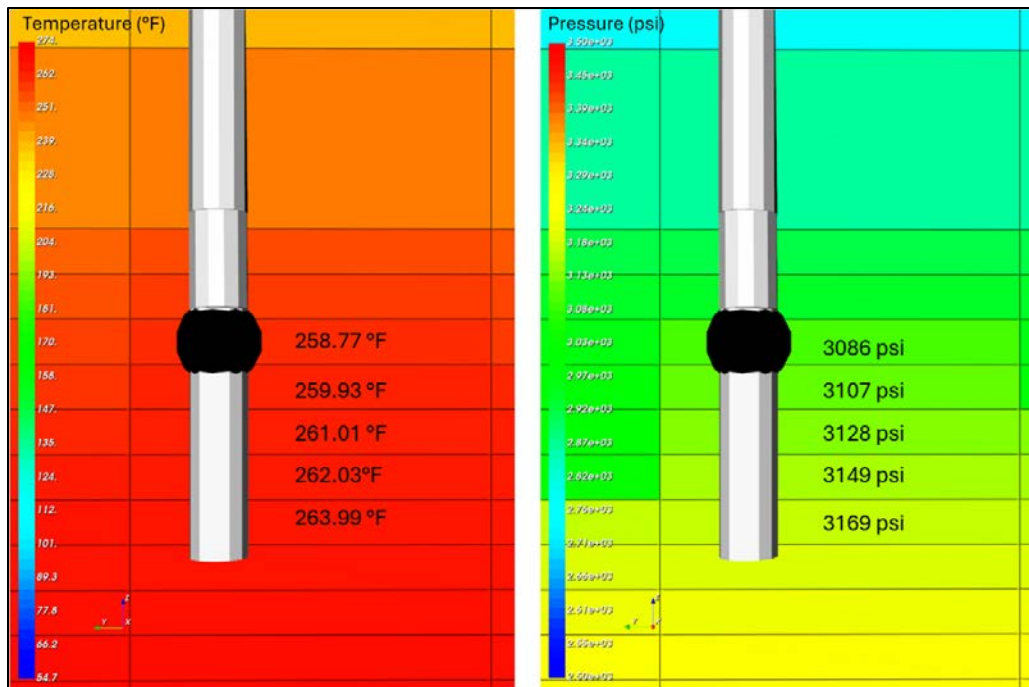
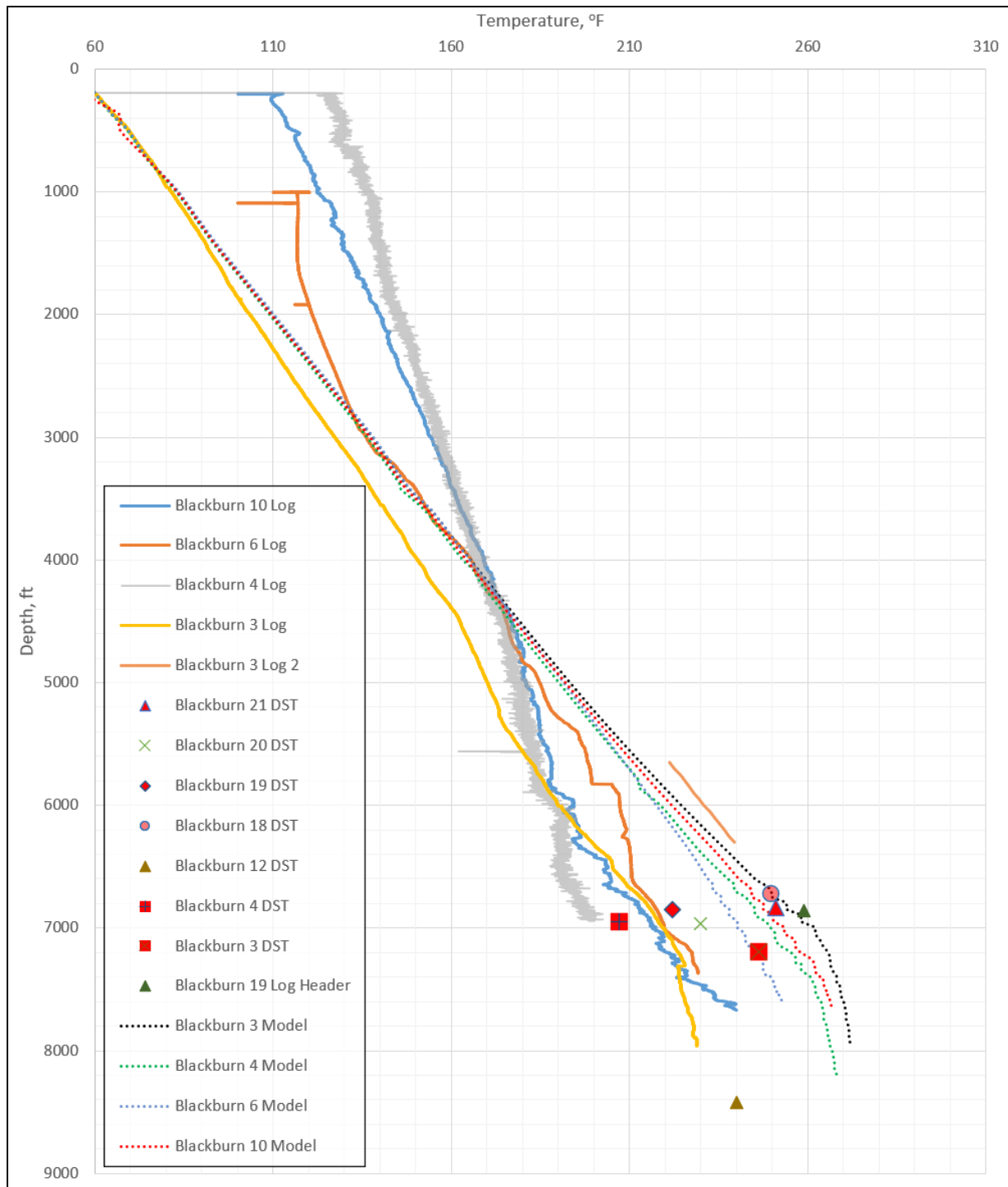


Figure 7: (Left) Modeled temperatures at the center of each grid cell along the Blackburn No. 18 wellbore. (Right) Modeled pressures at the center of each grid cell along the Blackburn No. 18 wellbore. The black ellipsoid denotes the bottom of the tubing at 6,750 ft MD.

Modeled temperature profiles for Blackburn No. 3, 4, 6, and 10 are compared to historic well log temperature profiles in Figure 8. The first Blackburn No. 3 log was taken on March 23, 1982, one week after drilling stopped on March 16, 1982. The second Blackburn No. 3 log was taken July 1, 1982, an estimated 3 months after the well was completed and in production. All other logs were taken within days of completion or drilling: Blackburn No. 4 was taken 3 days after completion, No. 6 was taken 3 days after completion, and No. 10 was taken the day after total depth was reached.

The temperatures from these logs are likely not reflective of the actual subsurface thermal gradient because of post-drilling mud circulation: i.e., the top of the wellbore heats up when mud is circulated from deeper depths to the surface, and the bottom of the wellbore cools as mud is circulated from the surface to deeper depths. The second log of Blackburn No. 3 was suspected of being affected by production-related heating. Model profiles for Blackburn No. 3, 4, 6, and 10 were generated from selecting the temperatures in the center of each calibrated reservoir grid cell along the respective well tracks. The modeled profiles show agreement with historic DST data collected for Blackburn No. 3, 18, 19 Log Header, and 21.



**Figure 8: Stabilized temperature profiles modeled by the static reservoir simulation for Blackburn No. 3, 4, 6, and 10 shown alongside historic well log and DST data.**

### ***3.3 Production Modeling***

The objective of the dynamic reservoir modeling was to simulate production/injection scenarios being considered for field deployment. The focus of this part of the study was to determine whether

detrimental thermal breakthrough or pressure depletion would be present during the lifetime of the project.

Three dynamic production scenarios were selected to simulate production and injection well schemes. These scenarios were chosen mainly to determine the co-production water rate that the Blackburn field can support while considering operational constraints associated with the ongoing oil production. A summary of the scenario details is shown in Table 3. An overview of the well locations with respect to the reservoir is shown in Figure 9. All scenario flow rate inputs were converted from volumetric rate to mass rate using a density of 947.7 kg/m<sup>3</sup>; this value represents the density of pure water at 260°F and 3,000 psi.

**Table 3: Summary of dynamic production scenarios. All wells denoted with numbers alone are Blackburn Field wells.**

Scenario	Producing Wells	Injecting Wells	Total Production	Total Injection
			BPD	BPD
1	16, 18, 19	12, 21	14,200	14,200
2	16, 18, 19, 22	12, 21	24,200	24,200
3	4, 16, 18, 19, 22	12, 20, 21; Bucy No. 1	34,200	34,200

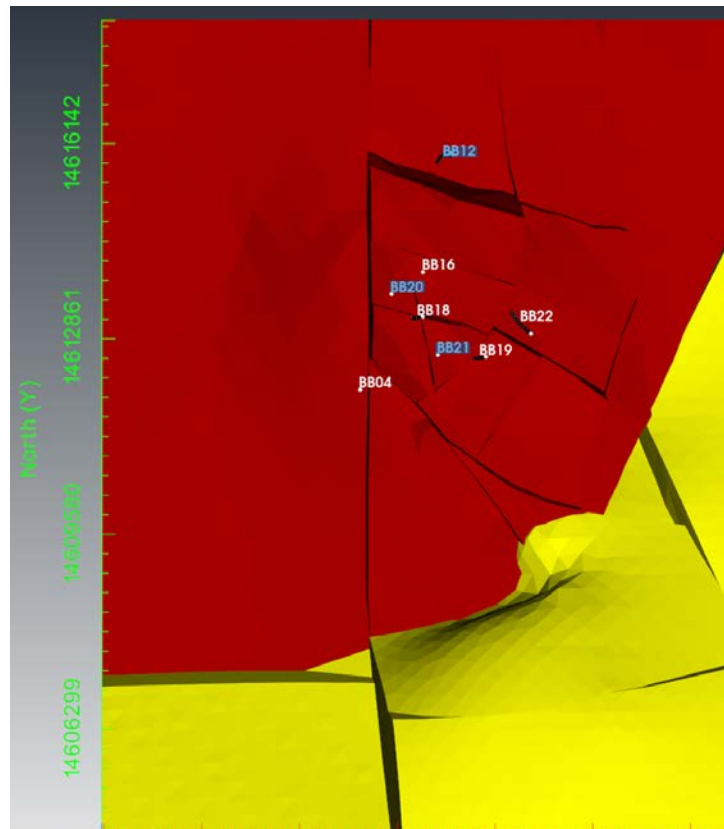


**Figure 9: Scenario wells imposed on the geological model. Rock formations depicted in red and yellow colors represent the Nevada and the quartz monzonite formations, respectively. Injector well names are highlighted with blue.**

Injection temperatures for scenarios depended on the surface operations and losses encountered at the surface. We assumed a fixed reinjection temperature of 179°F for all scenarios based on ORC performance analysis done by Gradient Geothermal, Inc. We did not incorporate Bucy No. 1’s injection into the model because it is located outside the model domain.

The production wells were fully implemented into the numerical simulator to calculate the pressure and temperature changes along the wells. The injection wells were abstracted in the reservoir model by implementing mass sources located in the numerical grid, coinciding with the bottom-hole locations of the injection wells.

To develop wellbore geometry (hole and tubular dimensions), we used our best estimation from well completion reports and reports from the Blackburn field operator (publicly hosted by NBMG, 2023). Well completion reports were most heavily relied upon, because they offered the most comprehensive understanding of the well geometries. Regarding work not included in the well completion reports, specifically deepening of wells, the information obtained from Gradient Geothermal, Inc. and the operator was relied on.

### 3.3.1 Scenario 1

The details of this co-production scenario were as follows:

- The total production is 14,200 BPD.
- The total injection is 14,200 BPD.
- The combined production target temperature is 250°F.

**Table 4: Summary of Scenario 1 dynamic production scheme. All wells denoted with numbers alone are Blackburn Field wells.**

Scenario	Producing Wells	Injecting Wells	Target Flow Rate
			BPD
1	16	-	10,000
	18	-	2,100
	19	-	2,100
	-	12	10,000
	-	21	4,200

The flow rates stated above were incorporated into the respective production wells and injection mass sources in the Brynhild reservoir simulator. Figure 10 presents the temperature behavior of the produced fluids in respective scenario wells. A volumetric rate-weighted combined average temperature was also calculated.

In this scenario, the combined production temperature was 262.4°F at the end of four years, and the average of the combined production temperature was 262.5°F during this period. At the end of the ten-year production period, the combined production temperature was 261.8°F. No significant thermal decline was observed. The design target temperature of 250°F was met. The reservoir pressure support was sufficient to sustain flow naturally at the production wells within the simulated timeframe.



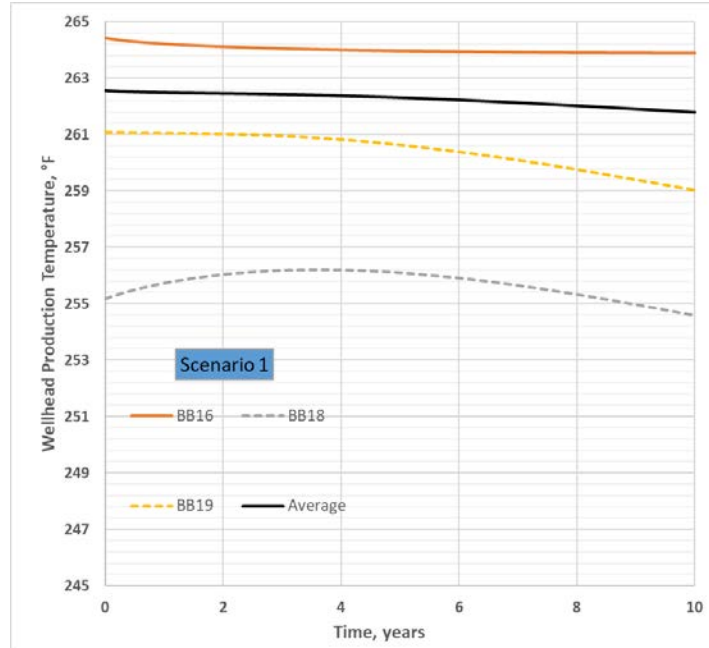


Figure 10: Wellhead production temperatures associated with Scenario 1. The black line represents the volumetric weighted average production temperature. BB denotes Blackburn wells.

### 3.3.2 Scenario 2

The details of this co-production scenario were as follows:

- The total production is 24,200 BPD.
- The total injection is 24,200 BPD.
- The combined production target temperature is 260°F.

Table 5: Summary of Scenario 2 dynamic production scheme. All wells denoted with numbers alone are Blackburn Field wells.

Scenario	Producing Wells	Injecting Wells	Target Flow Rate
			BPD
2	16	-	10,000
	18	-	2,100
	19	-	2,100
	22	-	10,000
	-	12	12,100
	-	21	12,100

The flow rates stated above were incorporated into the respective production wells and injection mass sources in the Brynhild reservoir simulator. Figure 11 presents the temperature behavior of the produced fluids in respective scenario wells. In this scenario, the combined production temperature was 262.7°F at the end of four years, and the average of the combined production temperature was 263.0°F during this period. At the end of the ten-year production period, the combined production temperature was 260.8°F. The design target temperature of 260°F was met.

The reservoir pressure support was sufficient to sustain flow naturally at the production wells within the simulated timeframe.

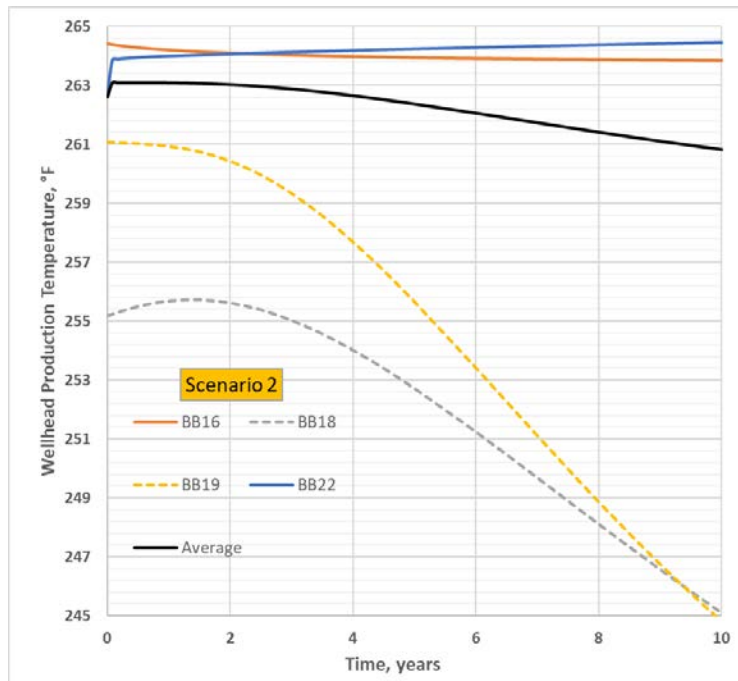


Figure 11: Wellhead production temperatures associated with Scenario 2. The black line represents the volumetric weighted average production temperature. BB denotes Blackburn wells.

### 3.3.3 Scenario 3

The details of this co-production scenario were as follows:

- The total production is 34,200 BPD.
- The total injection is 34,200 BPD.
- The combined production target temperature is 270°F.

Table 6: Summary of Scenario 3 dynamic production scheme. All wells denoted with numbers alone are Blackburn Field wells.

Scenario	Producing Wells	Injecting Wells	Target Flow Rate
			BPD
3	4	-	10,000
	16	-	10,000
	18	-	2,100
	19	-	2,100
	22	-	10,000
	-	12	8,550
	-	20	8,550
	-	21	8,550
-	-	Bucy No. 1	8,550

The flow rates stated above, except Bucy No. 1, were incorporated into the respective production wells and injection mass sources in the Brynhild reservoir simulator. Bucy No. 1 is located 0.6 mi NNW of Blackburn No. 12 and hence is located outside the constructed geological (and hence the reservoir) model. Our model analysis showed that Blackburn No. 12's reinjection did not affect the production wells in all scenarios. The fluids injected at this location predominantly sank down to the constant pressure boundary condition because of the density contrast of the injected fluid. We concluded that, similar to Blackburn 12, injection at Bucy No. 1 would not induce a significant temperature drop at the modeled production wells because of its location.

Figure 12 presents the temperature behavior of the produced fluids in respective scenario wells. In this scenario, the combined production temperature was 262.0°F at the end of four years, and the average of the combined production temperature was 262.1°F during this period. At the end of the ten-year production period, the combined production temperature was 259.5°F. The target production temperature of 270°F was not met. The reservoir pressure support was sufficient to sustain flow naturally at the production wells within the simulated timeframe. Compared to Scenario 2, there is less thermal decline in Blackburn 18 and 19; however, cooling was also observed at Blackburn 16 because of the injection at Blackburn 20, which was only active in this scenario.

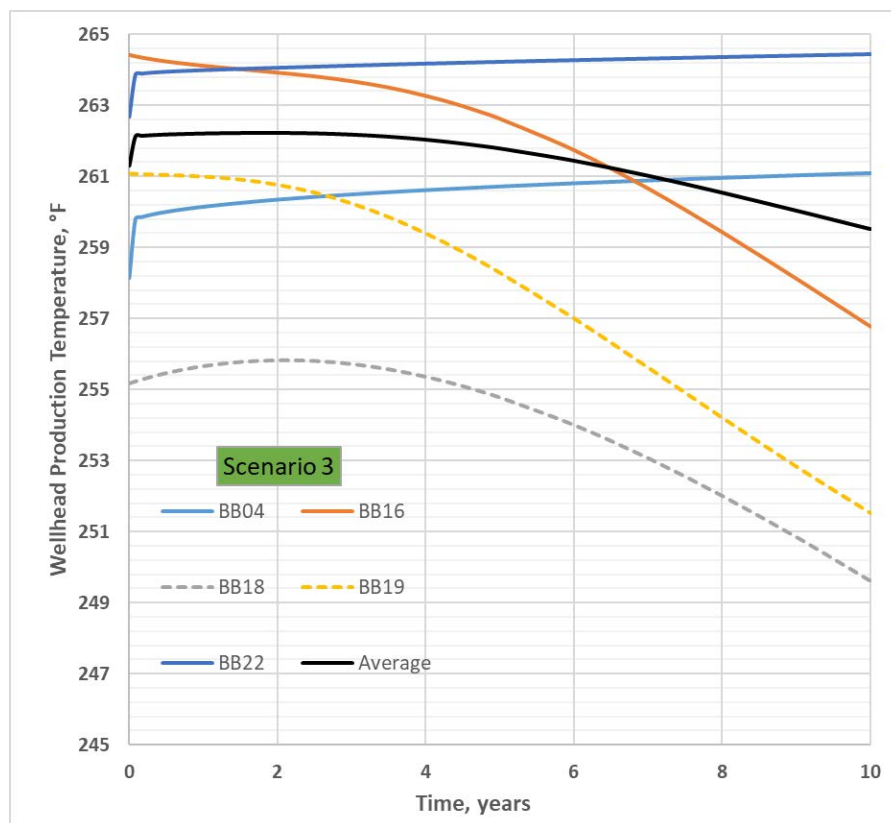


Figure 12: Wellhead production temperatures associated with Scenario 3. The black line represents the volumetric weighted average production temperature. BB denotes Blackburn wells.

### 3.3.4 Scenario Summary

Presented below are tabulated and graphical summaries of the combined temperatures associated with the three design scenarios, for quick reference.

**Table 7: Combined production temperature values associated with three design scenarios.**

Scenario	Combined Production Temperature Statistics			
	4-Year Term		10-Year Term	
	End of Term, °F	Term Average, °F	End of Term, °F	Term Average, °F
1	262.4	262.5	261.8	262.4
2	262.7	263.0	260.8	262.7
3	262.0	262.1	259.5	261.9

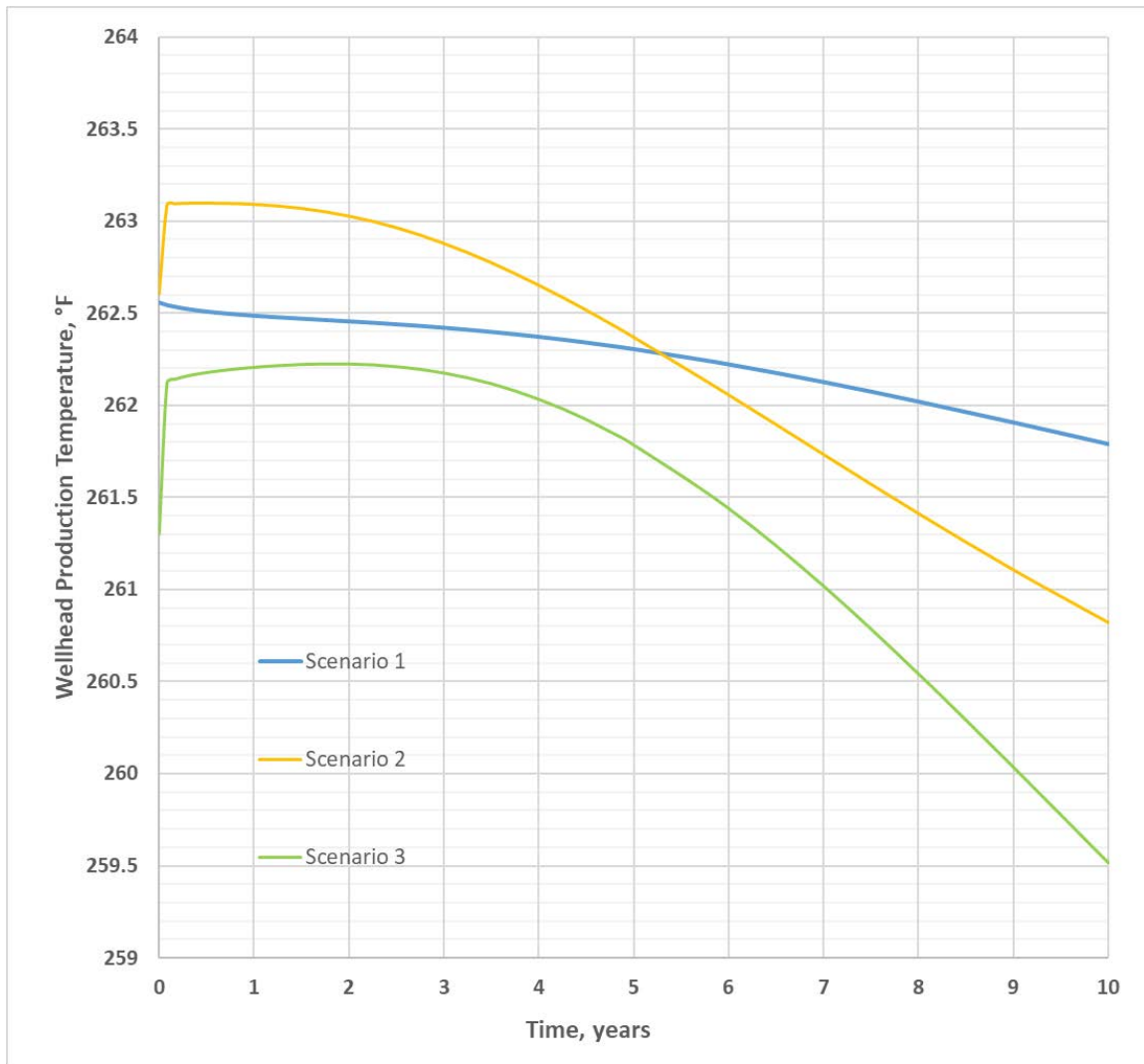


**Figure 13: Combined production temperatures associated with three simulated design scenarios.**



## 4. Conclusions

This study presents the results of geological and reservoir modeling work done to support the feasibility analysis study of geothermal co-production at the Blackburn Oil Field. We simulated three production scenarios in the numerical reservoir model. The three scenarios indicate negligible to minimal thermal decline over the duration of a simulated 10-year production and re-injection scheme. The first and second scenarios matched respective production temperature targets. Simulations for the third scenario showed that a target combined production temperature of 270°F cannot be achieved. The first production scenario is the likely deployment candidate for the second phase of the WOO Nevada project. Planned future work for the second phase includes technical design support and data collection from field tests.

## Acknowledgement

This work was authored by the National Renewable Energy Laboratory, operated by Alliance for Sustainable Energy, LLC, for the U.S. Department of Energy (DOE) under Contract No. DE-AC36-08GO28308. Funding was provided by the U.S. Department of Energy Office of Energy Efficiency and Renewable Energy Geothermal Technologies Office. The views expressed herein do not necessarily represent the views of the DOE or the U.S. Government. The U.S. Government retains, and the publisher, by accepting the article for publication, acknowledges that the U.S. Government retains a nonexclusive, paid-up, irrevocable, worldwide license to publish or reproduce the published form of this work, or allow others to do so, for U.S. Government purposes. We would like to thank our collaborators at Transitional Energy (now Gradient Geothermal) for their continued support and dedication to this project.

## REFERENCES

- Blackwell, D. D., & Steele, J. L. (1989). Thermal Conductivity of Sedimentary Rocks: Measurement and Significance. In N. D. Naeser & T. H. McCulloh (Eds.), *Thermal History of Sedimentary Basins*, pp. 13–36. Springer New York. [https://doi.org/10.1007/978-1-4612-3492-0\\_2](https://doi.org/10.1007/978-1-4612-3492-0_2)
- Faulds, J. E., Hinz, N. H., Dering, G. M., & Siler, D. L. (2013). The Hybrid Model—The Most Accommodating Structural Setting for Geothermal Power Generation in the Great Basin, Western USA. *Geothermal Resources Council Transactions* 37:3-10.
- Faulds, J. E., Coolbaugh, M. F., Vice, G. S., & Edwards, M. L. (2006). Characterizing structural controls of geothermal fields in the northwestern Great Basin: A progress report. 30, pp. 69–76. *Geothermal Resources Council Transactions*.
- Fetoui, I. (2017, October 18). Tubing Specifications. *Production Technology*. <https://production-technology.org/tubing-specifications/>
- Flanigan, T.E., 1994. The Blackburn Oil Field: Oil, above a low-angle detachment fault in Eureka County, Nevada. In Schalla, R.A., and Johnson, E.H. (eds.), *Oil fields of the Great Basin*, Nevada Petroleum Society, p. 380.

- Garside, L.J., Hess, R.H., Fleming, ICL., and Weimer, B.S. (1988). Oil and gas developments in Nevada. Nevada Bureau of Mines and Geology, Bulletin 104, p. 136.
- Hulen, J. B., Bereskin, R. S., & Bortz, L. C. (1990). High-Temperature Hydrothermal Origin for Fractured Carbonate Reservoirs in the Blackburn Oil Field, Nevada. *The American Association of Petroleum Geologists*, 74(2), p. 1262–1272.
- Kutun, K., Gold, A., & Beckers, K. (2023). Resource Characterization to Estimate Potential for Electricity Co-Production at Blackburn Oil Field, Nevada. 2498-2514. Paper presented at 2023 Geothermal Rising Conference, Reno, Nevada.
- Manger, G. E. (1963). Porosity and bulk density of sedimentary rocks (No. 1144-E). USGPO.
- Nevada Division of Minerals (2023). Nevada Division of Minerals Open Data Site. <https://data-ndom.opendata.arcgis.com/>
- Nevada Bureau of Mines and Geology (NBMG). (2023). Oil and Gas Well Log Files. (Database). Nevada Bureau of Mines and Geology. <https://nbgm.unr.edu/oil&gas/WellSearch.html>
- NRCS NWCC Report Generator—Ruby (2229) Nevada SCAN Site—6000 ft (NRCS). (12 Mar. 2024). National Resources Conservation Service. [wcc.sc.egov.usda.gov/reportGenerator/](http://wcc.sc.egov.usda.gov/reportGenerator/)
- Sass, J. H., Lachenbruch, A. H., Dudley, W. W., Priest, S. S., & Munroe, R. J. (1988). Temperature, thermal conductivity, and heat flow near Yucca Mountain, Nevada: Some tectonic and hydrologic implications. (Open File). 87–649, p. 26). United States Department of the Interior Geological Survey.
- Schön, J.H. (Ed.) (2015) *Physical Properties of Rocks: Fundamentals and Principles of Petrophysics*. *Developments in Petroleum Science*, 65. Elsevier.
- Schön, J.H. (2011). *Physical Properties of Rocks: A Workbook (Handbook of Petroleum Exploration and Production)*. Elsevier.
- Scott, C., & Chamberlain, A. K. (1988). The Blackburn Oil Field, Nevada: A Case History. *Rocky Mountain Association of Geologists Guidebook*, p.241-250. Denver, Colorado.
- Takacs, G. (2015). Chapter 2—A Review of Production Engineering Fundamentals. In G. Takacs (Ed.), *Sucker-Rod Pumping Handbook*. p. 13–56. Gulf Professional Publishing. <https://doi.org/10.1016/B978-0-12-417204-3.00002-9>
- Taverna, Nicole. (2019). Sedimentary Geothermal Feasibility in Eastern Nevada and Millard County, Utah Well Databases. (Database). <https://dx.doi.org/10.15121/1637461>
- U. S. Environmental Protection Agency (2016). National Elevation Dataset (30 m). (Dataset). [https://archive.epa.gov/esd/archive-nerl-esd1/web/html/nvgeo\\_gis3\\_dem.html#map](https://archive.epa.gov/esd/archive-nerl-esd1/web/html/nvgeo_gis3_dem.html#map)
- University of Nevada, Reno (UNR). (2021). INGENIOUS Thermal Conductivity Measurement Source Categorization. (Data set). Retrieved from <https://dx.doi.org/10.15121/1874222>.
- Waples, D. W., & Waples, J. S. (2004). A Review and Evaluation of Specific Heat Capacities of Rocks, Minerals, and Subsurface Fluids. Part 1: Minerals and Nonporous Rocks. *Natural Resources Research*, 13(2), p. 97–122. doi.org/10.1023/B:NARR.0000032647.41046.e7
- Zhu, X., Gao, Z., Chen, T., Wang, W., Lu, C., & Zhang, Q. (2022). Study on the Thermophysical Properties and Influencing Factors of Regional Surface Shallow Rock and Soil in China. *Frontiers in Earth Science*, 10, p. 1–13.